Developmental Cell
Article

Cleavage of TRPM7 Releases the Kinase Domain from the Ion Channel and Regulates Its Participation in Fas-Induced Apoptosis

Bimal N. Desai,[1,4,5] Grigory Krapivinsky,[1,4] Betsy Navarro,[1] Luba Krapivinsky,[1] Brett C. Carter,[2] Sebastien Febvay,[2] Markus Delling,[1] Anirudh Penumaka,[1] I. Scott Ramsey,[3] Yunona Manasian,[1] and David E. Clapham[1,2,*]
[1]Department of Cardiology, Howard Hughes Medical Institute, Manton Center for Orphan Disease, Children's Hospital Boston, Enders Building 1309, 320 Longwood Avenue, Boston, MA 02115, USA
[2]Department of Neurobiology, Harvard Medical School, Boston, MA 02115, USA
[3]Department of Physiology and Biophysics, Virginia Commonwealth University, Richmond, VA 23298, USA
[4]These authors contributed equally to this work
[5]Present address: Department of Pharmacology, University of Virginia School of Medicine, Charlottesville, VA 22908, USA
*Correspondence: dclapham@enders.tch.harvard.edu
DOI 10.1016/j.devcel.2012.04.006

SUMMARY

Transient receptor potential melastatin-like 7 (TRPM7) is a channel protein that also contains a regulatory serine-threonine kinase domain. Here, we find that Trpm7$^{-/-}$ T cells are deficient in Fas-receptor-induced apoptosis and that TRPM7 channel activity participates in the apoptotic process and is regulated by caspase-dependent cleavage. This function of TRPM7 is dependent on its function as a channel, but not as a kinase. TRPM7 is cleaved by caspases at D1510, disassociating the carboxy-terminal kinase domain from the pore without disrupting the phosphotransferase activity of the released kinase but substantially increasing TRPM7 ion channel activity. Furthermore, we show that TRPM7 regulates endocytic compartmentalization of the Fas receptor after receptor stimulation, an important process for apoptotic signaling through Fas receptors. These findings raise the possibility that other members of the TRP channel superfamily are also regulated by caspase-mediated cleavage, with wide-ranging implications for cell death and differentiation.

INTRODUCTION

Transient receptor potential melastatin-like 7 (TRPM7), a member of the TRPM subgroup of transient receptor potential (TRP) channels, is a large (1,862 aa, 210 kDa) protein that contains both a cation-conducting pore and a serine-threonine kinase—an unusual molecular configuration often referred to as a "chanzyme" for its channel-enzyme bifunctionality (Nadler et al., 2001; Runnels et al., 2001). TRPM7 is nonselective among cations but is permeant to and inhibitable by intracellular Mg^{2+} (Kozak and Cahalan, 2003; Nadler et al., 2001). Conducting only a few pA of inward current at physiological pH, it is potentiated at low extracellular pH (Jiang et al., 2005) and by phospholipase C-linked receptors in intact cells (Langeslag et al., 2007). *Trpm7*$^{-/-}$ embryos do not survive past day 7 of embryogenesis (Jin et al., 2008), indicating that TRPM7 has an essential and nonredundant role in mouse development. TRPM7 is expressed in all cell types examined (Kunert-Keil et al., 2006; Ramsey et al., 2006), and organ development is widely disrupted in tissue-specific Trpm7$^{-/-}$-deficient mice (Jin et al., 2012). Similarly, selective deletion of *Trpm7* in the T cell lineage disrupts thymocyte development and accelerates thymic involution (Jin et al., 2008).

TRPM7's carboxy-terminal kinase is homologous to a family of atypical serine-threonine kinases called α-kinases and is structurally similar to protein kinase A (PKA) (Yamaguchi et al., 2001). TRPM7 autophosphorylates at multiple sites and can phosphorylate annexin A1 (Dorovkov and Ryazanov, 2004) and myosin IIA heavy chain (Clark et al., 2008), although its natural substrates are not known. The proximity of the kinase domain to the Mg^{2+}-permeating but nonselective pore may be of significance to signal transduction, with TRPM7 mediating a localized cation flux (Ca^{2+}, Na^{+}, Mg^{2+}, and trace ions such as Zn^{2+}) either at the plasma membrane or via specialized intracellular vesicles. The kinase domain, in turn, has been proposed to be involved in mediating the inhibition of TRPM7 channel by serving as a binding site for Mg^{2+} and Mg^{2+}-bound nucleotides (Demeuse et al., 2006). Alternatively, because the K_D for Mg^{2+} inhibition of TRPM7 is ~0.6 mM (Nadler et al., 2001), near physiological levels of free Mg^{2+} (0.5 ± 0.2 mM) (Romani and Scarpa, 2000), and ATP is the primary regulator of free Mg^{2+}, TRPM7 may be a metabolic sensor. Environmental acidic pH (Jiang et al., 2005), high intracellular PIP_2 (Runnels et al., 2002), and high internal ATP levels (low free Mg^{2+}) should maximize TRPM7 channel activity. A proposed requirement of TRPM7 in vertebrate Mg^{2+} homeostasis (Ryazanova et al., 2010; Schmitz et al., 2003) is incongruent with the evidence that TRPM7 currents are small at physiological membrane potentials (<10 pA at −60mV), the recent identification of ubiquitous Mg^{2+} transporters (Li et al., 2011; Zhou and Clapham, 2009), and our finding that *Trpm7*$^{-/-}$ lymphocytes and other cell types are not deficient in acute Mg^{2+} uptake when exposed to extracellular 10 mM Mg^{2+}, or at steady state in total Mg^{2+} levels (Jin et al., 2008, 2012). Importantly, the Mg^{2+} permeability of TRPM7 may be of greater

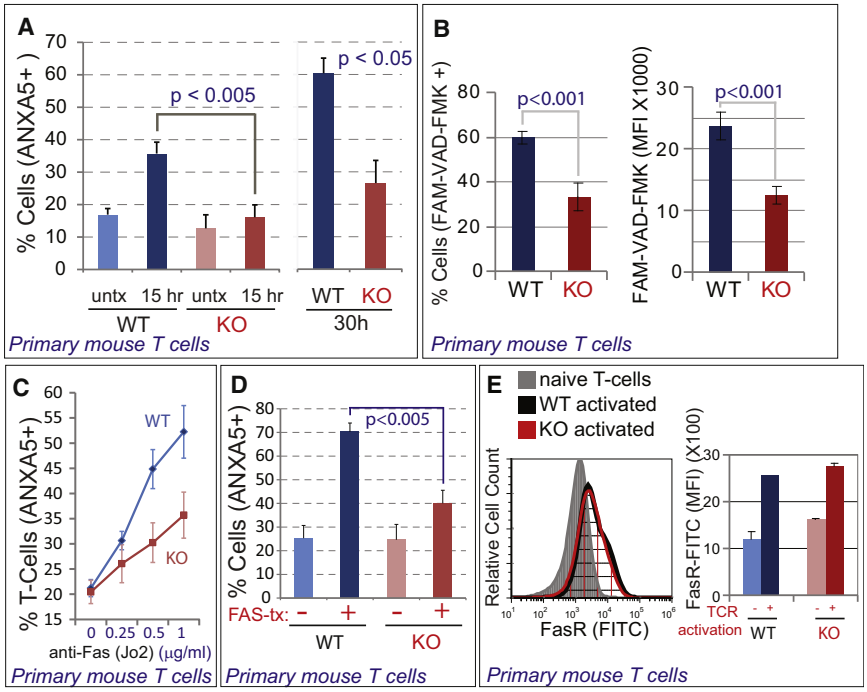

Figure 1. TRPM7-Deficient T Cells Are Deficient in Activation-Induced Apoptosis and Fas-Induced Apoptosis

(A) AICD measured by staining of WT (blue) and KO (red) T cells with annexin 5-Alexa 488 15 hr after stimulation. Bar graphs illustrate percentage of cells stained positive for cell-surface phosphatidylserine by ANXA5-Alexa 488 (ANXA5+) in unstimulated (untx) and cells stimulated with plate-bound anti-CD3 antibody for 15 hr (average ± SEM, n = 4). Right panel shows AICD after 30 hr of restimulation. Bar graphs present percentage of ANXA5+ cells after 30 hr of restimulation (±SEM, n = 4). Representative flow cytometry histograms are shown in Figure S1A.

(B) Reduced caspase activity in KO T cells 24 hr after restimulation with anti-CD3 and anti-CD28 antibodies. Bar graphs show percentage of cells with retained FAM-VAD-FMK (left) and mean fluorescence intensity (MFI) of FAM-VAD-FMK-positive T cells (right; ±SEM, n = 9).

(C) Detection of apoptosis by annexin A5 staining (ANXA5+) in WT (blue) and KO (red) T cells after Fas receptor stimulation with increasing concentrations of anti-Fas antibody (±SEM, n = 4). Representative flow cytometry histograms are shown in Figure S1B.

(D) Percentage of ANXA5+ T cells before and after Fas-induced apoptosis in WT (blue) and KO (red) T cells (plate-bound anti-Fas antibody; ±SEM, n = 4).

(E) Activation-induced cell surface upregulation of Fas or Fas receptor (FasR) as measured by staining with anti-FasR-FITC on activated WT T cells (black) and KO T cells (red) over typical naive T cells (gray). Bar graph illustrates average change in FasR-FITC expression on WT and KO T cells before and after activation (MFI of FasR-FITC staining; ±SD, n = 2).

See also Figure S1.

significance to intracellular signals that respond to highly localized intracellular Mg^{2+} around the intracellular mouth of TRPM7 channels.

Using *Trpm7*$^{fl/-}$ *(lck Cre)* mice (also referred to as *T*$^{M7-/-}$ mice) with selectively targeted deletion of *Trpm7* in the T cell lineage, we showed that TRPM7 is required for normal T cell development and that a large fraction of *Trpm7*$^{-/-}$ thymocytes arrest their thymic development at the DN3 stage, described by the cell surface immunophenotype CD4-CD8-CD44-CD25+ (Jin et al., 2008). The thymocytes that escape this developmental block, presumably by delayed deletion of *Trpm7*, survive and populate the peripheral lymphoid organs, albeit with a lower number of T cells. Interestingly, TRPM7 is deleted efficiently in these peripheral T cells (Jin et al., 2008), providing an opportunity to study TRPM7 in a postdevelopmental system. We have now investigated these peripheral *Trpm7*$^{-/-}$ T cells from *T*$^{M7-/-}$ mice in search of molecular mechanisms involved in the regulation and function of TRPM7. We show here that regulation of TRPM7 through caspase-mediated cleavage is important for Fas-induced apoptosis.

RESULTS

Trpm7$^{-/-}$ T Cells Show Markedly Reduced Activation-Induced Cell Death

In the process of studying T cell activation, we observed that in contrast to wild-type (WT) T cells, *Trpm7*$^{-/-}$ T cells do not show a substantial decrease in viability after T cell receptor (TCR) restimulation. Based on these observations, we investigated the phenomenon of activation-induced cell death (AICD), also referred to as restimulation-induced cell death (RICD), which results in the apoptosis of T cells upon repeated TCR stimulation (Green et al., 2003; Krammer et al., 2007). When actively growing WT T cells were restimulated with anti-CD3 antibodies, the percentage of annexin A5-positive (ANXA5+) cells increased from 15% to 35% after 15 hr of restimulation (Figure 1A; see Figure S1A available online). In contrast, AICD in *Trpm7*$^{-/-}$ T cells was significantly blunted (Figures 1A and S1A). The difference was also seen when AICD was measured after 30 hr of restimulation (Figures 1A and S1A). Accordingly, *Trpm7*$^{-/-}$ T cells are also deficient in activation of caspases as measured by FAM-VAD-FMK, a fluorescent cell-permeable probe of caspase activity (Figure 1B). Because AICD is dependent on death-receptor signaling (Krammer et al., 2007), we tested the sensitivity to Fas-induced apoptosis in *Trpm7*$^{-/-}$ T cells.

Trpm7$^{-/-}$ T Cells Are Defective in FAS Receptor-Induced Apoptosis

Actively growing T cells were stimulated with anti-Fas agonist antibody and crosslinking agent, Protein G, and the resulting apoptosis was measured by ANXA5 staining (Figure 1C). Flow cytometric histograms representing the increase in the percentage of ANXA5+ cells in response to increasing concentrations of anti-Fas agonist antibody are shown as overlays of WT and *Trpm7*$^{-/-}$ (KO) T cells (Figure S1B). These results indicate that *Trpm7*$^{-/-}$ T cells are significantly less sensitive to

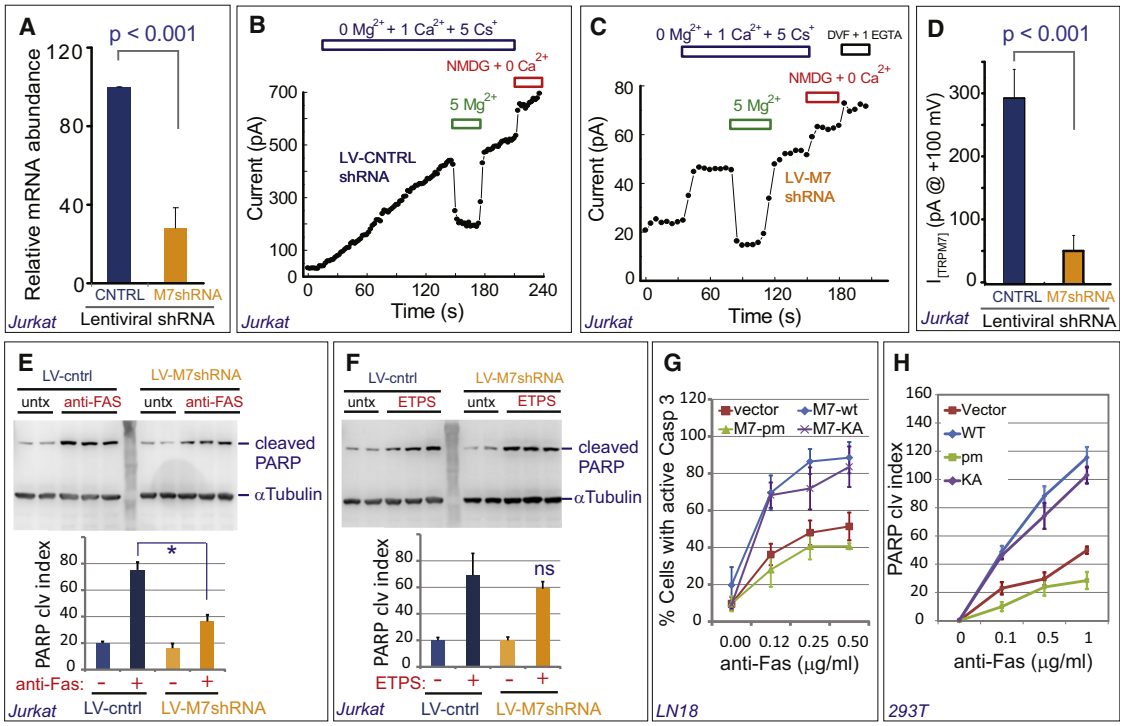

Figure 2. TRPM7 Channel, but Not Kinase, Activity Participates in Fas-Induced Apoptosis

(A) Quantitative real-time PCR showing efficient *Trpm7* mRNA knockdown in Jurkat cells to ~30% of control (±SEM, n = 3).

(B) Native I_{TRPM7} in Jurkat cells infected with control lentiviral shRNA. Plotted are peak outward currents measured from repeated 300 ms ramps at 2 s intervals from −100mV to +100mV (see Figure S5 for details). Characteristically, I_{TRPM7} slowly increases after patch-pipette "break-in" and dialysis of intracellular Mg^{2+} out of the cell. Both the increase in current after break-in and its inhibition by perfusion with 5 mM Mg^{2+} are characteristic of I_{TRPM7}.

(C) I_{TRPM7} is reduced ~10-fold (compare to B; note y axis scale change) in Jurkat cell that had been infected with TRPM7-specific lentiviral shRNA.

(D) Summary of recordings (examples in B and C) showing that peak I_{TRPM7} is reduced by shRNA knockdown of TRPM7 to 16% of control (CNTRL) (I_{TRPM7} at +100mV; ±SEM, n = 4).

(E) TRPM7 knockdown Jurkat cells are resistant to Fas-induced cell death. Immunoblots of cleaved PARP and α-tubulin in lysates of unstimulated (untx, n = 2) and Fas-stimulated (anti-Fas, n = 3) Jurkat cells infected with control (blue) and TRPM7-specific shRNA (orange). The PARP cleavage index (average ± SEM) (bottom) was calculated using the densitometric ratio of cleaved PARP signal over α-tubulin.

(F) TRPM7 knockdown Jurkat cells were not resistant to etoposide-induced cell death (25 μM, 8 hr). Bottom shows PARP cleavage index of etoposide-induced apoptosis in Jurkat cells infected with the control and M7shRNA-expressing lentivirus.

(G) Fas sensitivity of LN18 cells expressing variants of TRPM7 as evaluated by dose-dependent increase in percentage of LN18 cells with active caspase-3 (±SD, n = 3). The transfected variants include WT, nonconducting pore mutant (pm), and the kinase-dead K1646A (KA) mutant. Cells were stimulated with anti-Fas antibody for 3 hr prior to fixation and immunostaining. The percentages of apoptotic cells were calculated as cells exhibiting activated caspase-3 divided by transfected (RFP+) cells.

(H) Apoptosis induced by increasing concentrations of anti-Fas antibody in 293T cells cotransfected with TRPM7 variants. Fas-induced apoptosis was assessed by quantifying PARP cleavage in cell lysates. Data points represent the corresponding average PARP-cleavage indices (±SEM, n = 4).

See also Figure S2 and Movie S1.

Fas-stimulated apoptosis throughout the effective range of the agonist antibody concentration. We also evaluated WT and mutant T cell sensitivity to plate-bound anti-Fas agonist antibody and confirmed the relative resistance of *Trpm7*$^{-/-}$ T cells to Fas-induced apoptosis (Figure 1D). These findings are consistent with cell viability assays in response to Fas stimulation (Figure S1C). The cell surface levels of Fas receptor on activated *Trpm7*$^{-/-}$ T cells were equal to WT T cells (Figure 1E).

Resistance to Fas-Induced Cell Death after Depletion of TRPM7 in Jurkat Cells

Next, we evaluated Fas-induced cell death in the human Jurkat T cell leukemia cell line using an RNAi approach. To deplete TRPM7 levels in Jurkat cells, we generated a lentivirus that expresses a small hairpin RNA directed against the TRPM7 mRNA (LV-M7shRNA) and also marks the transduced cell through bicistronically expressed GFP. The resulting depletion of TRPM7 mRNA was evident by quantitative real-time PCR (Figure 2A). Patch-clamp recordings of GFP+ cells confirmed an ~10-fold reduction in the whole-cell TRPM7 current, I_{TRPM7} (Figures 2B–2D). We measured apoptosis in Jurkat cells by immunoblotting the lysates for cleaved Poly-ADP ribose polymerase (PARP), a terminal substrate of executioner caspases. Jurkat cells transduced with LV-M7shRNA were resistant to Fas-receptor-dependent cell death (Figure 2E), but not to etoposide-induced cell death (Figure 2F), which relies on a different signaling mechanism for initiating apoptosis (Lowe et al., 1993). The sensitivity of Fas-induced apoptosis in Jurkat

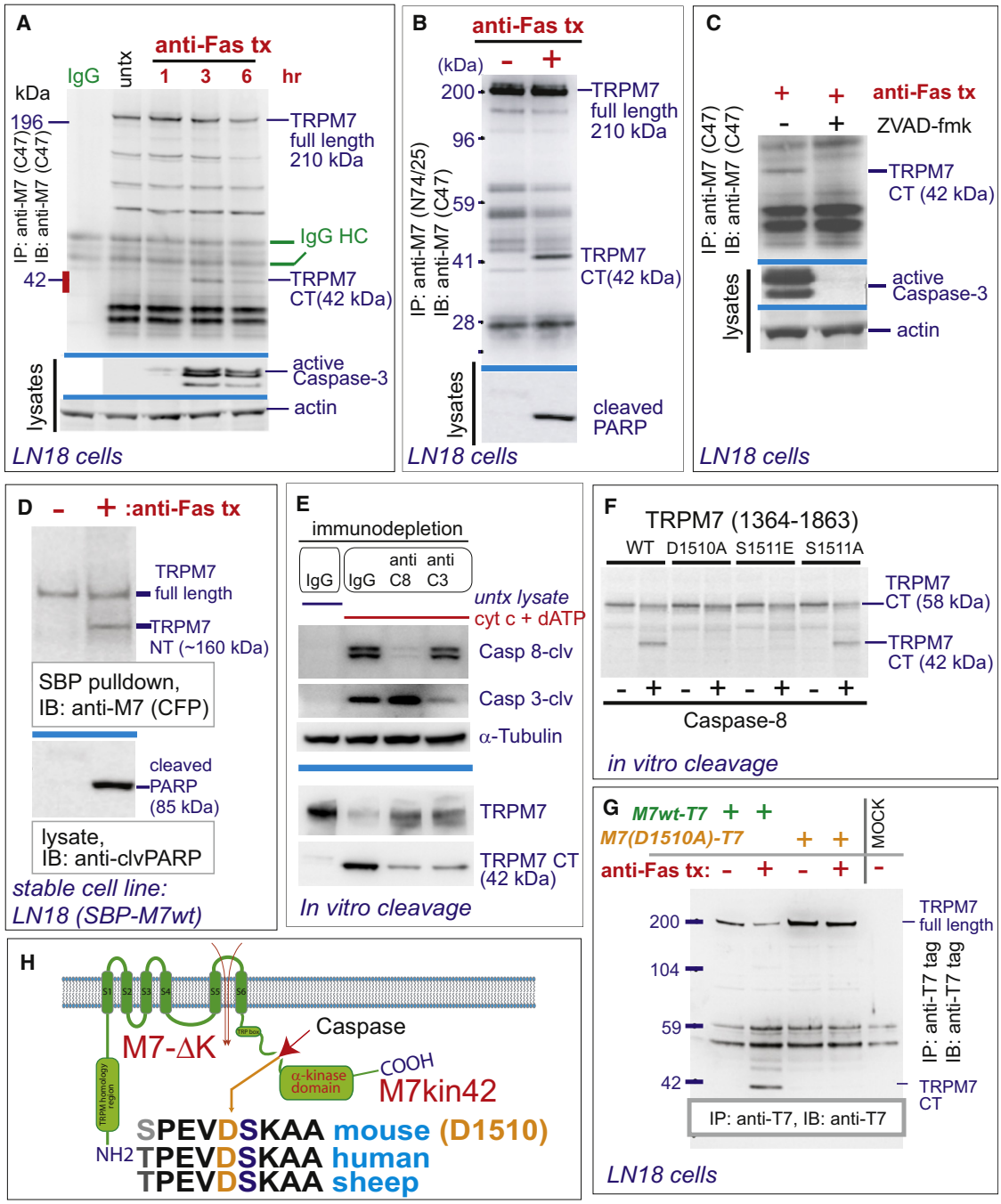

Figure 3. Fas Signaling Induces a Rapid Cleavage of TRPM7 in a Caspase-Dependent Manner

(A) LN18 cell Fas receptors were stimulated for the indicated times, and TRPM7 was immunoprecipitated using anti-TRPM7 (C47, raised against the TRPM7 kinase domain). The cleaved 42 kDa carboxy-terminus (CT) fragment is faintly detectable after 1 hr but robust at 3 hr after Fas receptor stimulation. Bottom panels present activation of caspase-3 as detected by immunoblotting with antibody specific for cleaved caspase-3 and actin

(B) Detection of the 42 kDa TRPM7 carboxy-terminal cleavage fragment using a mouse monoclonal antibody, N74/25, directed against the C-terminal amino acid sequence 1,817–1,863. The C-47 rabbit polyclonal antibody detected the fragment in the immunoblot. Bottom panels illustrate cleavage of PARP as detected by a cleaved PARP-specific antibody.

(C) Cleavage of TRPM7, as detected by appearance of the 42 kDa cleavage product, is abrogated when cells are treated with ZVAD-FMK (pan-caspase inhibitor) during 3 hr Fas receptor stimulation (same conditions used in A). Bottom shows activation of caspase-3 in the same samples.

(D) Fas-induced cleavage of TRPM7 yields an ~160 kDa N-terminal fragment (anti-M7 antibody generated against aa 1,277–1,380). Untreated and Fas-stimulated LN18 cells stably expressing N-terminal SBP-tagged TRPM7 were used to pull down M7 complexes using streptavidin beads prior to immunoblotting.

(E) Top shows in vitro activation of caspase-8 and caspase-3 in Jurkat S100 cytosolic extracts by addition of cytochrome *c* and dATP. In indicated samples, caspase-8 and caspase-3 were immunodepleted from the cytosolic extracts prior to activation by cytochrome *c* and dATP. Lower panel presents in vitro

T cells to depletion of TRPM7 supports the view that the defective Fas receptor signaling in *Trpm7*$^{-/-}$ T cells is not a result of a developmental defect. These findings strongly suggest that TRPM7 participates in Fas receptor signaling.

TRPM7 Potentiates Fas Receptor-Induced Activation of Caspase-3 in a Channel-Dependent and Kinase Activity-Independent Manner

For mechanistic insight, we set out to distinguish the relative contributions of the TRPM7 pore from its kinase activity in Fas receptor signaling. Because we failed to express TRPM7 variants with substantial efficiency in Jurkat cells, we screened for Fas-sensitive cell lines that enable the ectopic expression of TRPM7, a protein that is difficult to express transiently in most cell lines. LN18, an adherent human glioblastoma cell line, can express full-length variants of TRPM7 at an efficiency of 5%–10%. In these cells, Fas receptor signaling can be evaluated through immunofluorescent detection of the cleaved caspase-3 (active caspase-3), 3 hr after Fas stimulation (Figure S2E). Additional characterization of LN18 cells showed that these cells belong to the type 2 category of Fas-sensitive cells reliant on the mitochondrial amplification loop for the efficient completion of apoptosis. LN18 cells release cytochrome *c* in response to Fas activation, and ectopic expression of Bcl-2 reduces their sensitivity to Fas-induced apoptosis as detected by the percentage of cells with active caspase-3 (Figure S2A). Next, we confirmed that LN18 cell Fas sensitivity is affected by TRPM7 function. Transfection of LN18 cells with siRNA duplexes directed against the TRPM7 mRNA (M7siR#3) results in a substantial depletion of TRPM7 mRNA as measured by quantitative real-time PCR (Figure S2B). Testing these cell populations for Fas-induced apoptosis showed that depletion of TRPM7 in LN18 cells leads to reduced sensitivity to Fas-induced apoptosis as detected by the percentage of cells with active caspase-3 (Figure S2C).

Next, we evaluated the Fas sensitivity of LN18 cells. TRPM7 variants were expressed through a previously described plasmid, Red-pTracer-CAG (Brauchi et al., 2008), that bicistronically encodes monomeric RFP in transfected cells (Figure S2D). We confirmed that RFP+ cells also expressed the encoded TRPM7 variant (Figure S2D). When compared to LN18 cells transfected with vector alone, expression of WT TRPM7 (M7-WT) augments the activation of caspase-3 as measured 3 hr after Fas receptor stimulation (Figures 2G and S2E). In contrast, the ectopic expression of a TRPM7 variant with a mutant (nonconducting) pore (M7-pm) (Krapivinsky et al., 2006) does not affect caspase-3 activation. A TRPM7 variant with the amino acid substitution, K1646A, renders the kinase inactive (Matsushita et al., 2005), but it augmented Fas receptor signaling in a manner comparable to WT TRPM7 (Figure 2G). Similar results were obtained in 293T cells, which provide an avenue for high transfection efficiency. Because 293T cells express very low levels of Fas and are insensitive to Fas stimulation, the assay was carried out by sequentially expressing the Fas receptor and the TRPM7 variants. In this experiment, the Fas-induced apoptosis was measured by quantitative immunoblotting of cleaved PARP and α-tubulin (Figures 2H and S2G). The cleavage of PARP has been quantified by deriving the densitometric ratio of cleaved PARP and α-tubulin detected in the same immunoblot. These results show that ectopic expression of TRPM7-WT and TRPM7-KA, but not TRPM7-pm, potentiates Fas-induced cell death (Figure 2H). The expression of TRPM7 variants and Fas in these cells is shown in Figure S2H. Ectopic expression of M7-WT or M7-pm did not affect the expression or localization of coexpressed Fas (Figure S2H; data not shown). Interestingly, ectopic expression of TRPM7 in LN18 cells also potentiates TRAIL-induced apoptosis but does not have a substantial effect on apoptosis induced by exposure to UV light, etoposide, and staurosporine (Figure S2F). Overall, these results indicate that the role of TRPM7 in extrinsic apoptosis is dependent on the channel activity of TRPM7 and does not depend on its kinase activity.

TRPM7 Is Cleaved by a Caspase in Response to Fas Receptor Stimulation

Although TRPM7 current (I_{TRPM7}) is readily detectable in most cells, the TRPM7 protein is expressed at very low levels and is biochemically detectable by immunoblotting only after enrichment through immunoprecipitation. Compared to unstimulated LN18 cells, the Fas-stimulated LN18 cells contain a 40–42 kDa TRPM7 fragment that is detectable by immunoblotting with an antibody raised against the carboxy-terminal kinase domain of TRPM7 (Figure 3A). The emergence of this fragment is evident 1 hr after Fas ligation (Figures 3A and S3) and peaks 3 hr after Fas ligation. To rule out artifacts due to antibody cross-reactivity, we confirmed the cleavage using a different TRPM7 antibody for immunoprecipitation of endogenous TRPM7 (Figure 3B). When LN18 cells were treated with a pan-caspase inhibitor, ZVAD-fmk, the cleavage was abolished, indicating a dependence on caspase activity (Figure 3C). The anti-TRPM7 antibodies used in these immunoblots are reactive to the extreme carboxy-terminal amino acid sequence of TRPM7, indicating that the 42 kDa fragment of TRPM7 retains the carboxyl terminus kinase domain of TRPM7. We also generated a stable cell line of LN18 expressing a TRPM7 variant that was tagged at the N terminus with streptavidin-binding peptide (SBP). After Fas-induced TRPM7 cleavage, we pulled down the N-terminal fragment by using streptavidin beads and immunoblotted TRPM7 using a rabbit polyclonal antibody that was generated against the

cleavage of immunopurified TRPM7 by S100 extracts shown in top panel. TRPM7 was detected by anti-M7 antibody directed against the TRPM7 carboxy-terminus. Note the loss of full-length TRPM7 and emergence of the 42 kDa kinase domain upon cleavage.

(F) In vitro caspase-8 cleavage of TRPM7 is blocked by amino acid substitutions D1510A and S1511E. Mutation S1511A does not prevent cleavage of the ^{35}S-labeled TRPM7 C-terminal polypeptide.

(G) The TRPM7(D1510A) variant is not cleaved in vivo in response to Fas stimulation. LN18 cells were transfected with C-terminal T7-tagged variants of TRPM7 WT and TRPM7 (DA). Anti-T7 immunoprecipitates were probed for cleavage by immunoblotting with anti-T7 antibody to detect the 42 kDa C-terminal cleavage fragment.

(H) An illustration showing the dissociation of the TRPM7 channel and kinase domains after cleavage at D1510. The proximal sequence of the TRPM7 cleavage site in mouse, human, and sheep is shown.

See also Figure S3.

TRPM7 amino acid sequence 1,277–1,380 (N-terminal to the cleavage site D1510). This analysis shows the generation of an ~160 kDa N-terminal fragment of TRPM7 in Fas-stimulated cells (Figure 3D).

Caspase-8, as well as Caspase-3, Contributes to the Cleavage of TRPM7

Because TRPM7 cleavage was detectable 1 hr after Fas stimulation, we reasoned that the cleavage was mediated by caspase-8, the apical or initiator caspase during Fas-induced apoptosis. Inhibitors of caspase-8, however, are not useful in illuminating this aspect because inhibition of the initiator caspase prevents the activation of all subsequent caspases. To gain insight, we took advantage of a cell-free system that allows the activation of caspases in vitro through the addition of cytochrome *c* and dATP to cytosolic extracts (Li et al., 1997; Liu et al., 1996). Although this type of activation is initiated through the activation of apoptosome (Apaf-1-cytochrome *c*-caspase-9 complex), it leads to a comprehensive activation of caspases (including caspase-8) through a physiologically relevant, albeit in vitro, process that does not involve Fas signaling (McStay et al., 2008). We investigated the effect of immunodepletion of caspase-8 and caspase-3 on the in vitro cleavage of TRPM7 by such cytosolic preparations. When caspases in the cytosolic S100 preparations from Jurkat cells were activated by the addition of cytochrome *c* and dATP, the activated (cleaved) forms of caspase-8 and caspase-3 were readily detected (Figure 3E). In contrast, immunodepletion of caspase-3 and caspase-8 prior to activation by cytochrome *c* and dATP resulted in near-complete loss of these caspases in the activated preparations (Figure 3E). We then used these preparations to cleave immunopurified TRPM7 in vitro. As shown in Figure 3E (bottom), cleavage of TRPM7 is reduced by immunodepletion of caspase-8. However, we also find a similar reduction upon immunodepletion of caspase-3, indicating that caspase-8 contributes to TRPM7 cleavage but is not the exclusive mediator of TRPM7 cleavage. In the experiments discussed below, the in vitro cleavage of TRPM7 by caspase-8 is also demonstrated using purified caspase-8 (Figure 3F).

TRPM7 Is Cleaved at D1510, Releasing the Kinase Domain

Based on the molecular size of the TRPM7 carboxy-terminal cleavage fragment (~40 kDa), we reasoned that the TRPM7 cleavage site was approximately 350 aa upstream of the terminal amino acid and identified putative sequences that could serve as caspase substrates. The residue D1510 (mouse TRPM7 sequence) is flanked by a sequence that is congruent with the experimentally determined substrate selectivity of caspase-8 (Mahrus et al., 2008; Pop and Salvesen, 2009). In an in vitro assay of TRPM7 cleavage, using an ^{35}S-labeled 58 kDa C-terminal fragment of TRPM7 as the substrate, we confirmed that the caspase-8-mediated cleavage generates a 40–42 kDa C-terminal fragment (Figure 3F). Substitution of D1510 to an alanine (D1510A) abrogated the cleavage, suggesting that the cleavage occurred at D1510 (Figure 3F). Because the adjoining residue, S1511, is known to be autophosphorylated by TRPM7 kinase (Matsushita et al., 2005), we evaluated the effect of a phosphomimetic substitution, S1511E, and its converse substitution, S1511A. The S1511E substitution abolished TRPM7 cleavage, but S1511A was cleaved efficiently (Figure 3F). These results indicate that TRPM7 is cleaved early during Fas receptor stimulation at D1510, resulting in the dissociation of TRPM7's kinase domain from its channel domain. The results from the S1511 substitutions suggest a possible role for phosphorylation in the regulation of caspase-dependent TRPM7 cleavage, with the important caveat that caspase-8 strongly prefers small uncharged residues in this position (P1′) (Pop and Salvesen, 2009). The cleavage of TRPM7 at D1510 is also demonstrated through the analysis of ectopically expressed TRPM7 variants containing a carboxy-terminal T7 immunoepitope tag (Figure 3G). In contrast to WT TRPM7, the TRPM7 variant with a D1510A mutation is not cleaved in response to Fas stimulation of LN18 cells (Figure 3G). These results indicate that Fas receptor signaling results in the cleavage of TRPM7.

Taken together, these data lead us to conclude that in response to Fas signaling, TRPM7 undergoes a caspase-mediated cleavage at D1510 to generate two distinct proteins: the TRPM7 channel and the TRPM7 kinase. Based on the observation that the cleavage is detectable in the early phase of apoptosis (1 hr after Fas stimulation), the immunodepletion experiments, and in vitro cleavage of TRPM7 by caspase-8, we propose that the cleavage is initiated by caspase-8 but sustained by downstream caspases during the entire process of apoptosis. In contrast, caspase-8 substrates like Bid (Li et al., 1998) and RIPK3 (Kaiser et al., 2011; Oberst et al., 2011) are thought to be cleaved selectively by caspase-8 during extrinsic apoptosis. The caspase-dependent cleavage of TRPM7 is illustrated in Figure 3H.

The Dissociated Kinase Domain of TRPM7 Retains Phosphotransferase Activity but Does Not Potentiate Fas Receptor Signaling

The cleavage of TRPM7 at D1510 releases the 42 kDa polypeptide containing the kinase domain (M7kin42) from the membrane-resident channel. As discussed earlier, the participation of TRPM7 in Fas-induced apoptosis is dependent on the channel activity, and not the kinase activity. In accord with this, we show that although the released 42 kDa fragment retains kinase activity, it does not modulate Fas-induced apoptosis. We tested whether the released kinase is capable of phosphotransferase activity by conducting in vitro kinase assays with ectopically expressed FLAG-tagged M7kin42. Autophosphorylation activity of M7kin42 in the presence of ^{33}P-labeled ATP was evaluated by autoradiography, and M7kin42 was found to be active (Figure 4A). In contrast, M7kin42GV, a variant of the M7 kinase domain with a targeted substitution (G1619V) in the ATP-binding pocket, showed minimal autophosphorylation, indicating that the phosphorylation was not a result of an endogenous kinase in the immunoprecipitate (Figure 4A). Both variants of M7kin42, WT and GV, are expressed at comparable levels (Figures 4A and S4A). LN18 cells transfected with M7kin42-WT or M7kin42-GV variants showed no appreciable difference in the Fas-induced activation of caspase-3 (Figures 4B and S4B). Next, we tested whether the cleavage of TRPM7 is necessary for its participation in Fas-induced apoptosis.

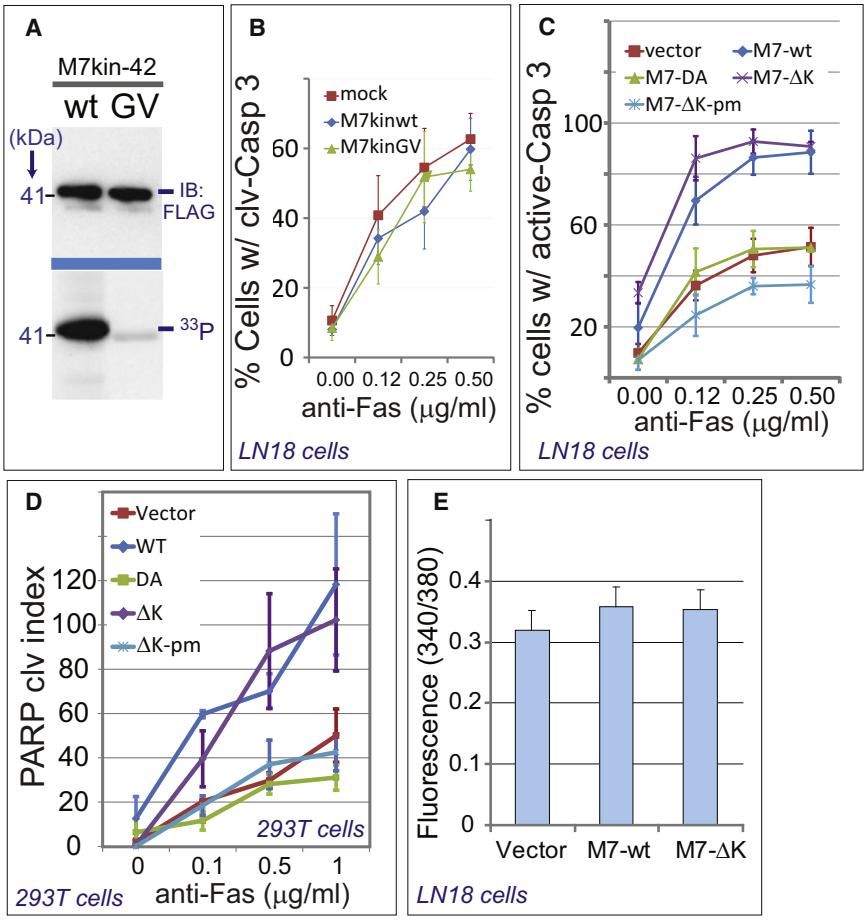

Figure 4. The Cleavage-Resistant Variant TRPM7(D1510A) Does Not Participate in Fas-Induced Apoptosis

(A) Phosphotransferase activity of FLAG-tagged M7kin42 and the kinase-dead variant, M7kin42 (GV), evaluated by in vitro autophosphorylation in the presence of ^{33}P-labeled ATP. Expression levels were confirmed by immunoblotting (IB) with anti-FLAG.

(B) Fas sensitivity of LN18 cells ectopically expressing the 42 kDa kinase fragment M7kin42 and its kinase-inactive variant, M7kin42(GV), in response to increasing concentrations of anti-Fas antibody (±SD, n = 2). clv, cleavage.

(C) Fas sensitivity of LN18 cells expressing TRPM7 variants as measured by the dose-dependent increase in the percentage of LN18 cells with active caspase-3 (WT, TRPM7-D1510A [DA, cleavage resistant], TRPM7-ΔK [cleaved], and TRPM7-ΔK-pm [cleaved, pore mutant]; ± SD, n = 3). Cells were stimulated with anti-Fas antibody for 3 hr prior to fixation and immunostaining. Apoptotic cells were calculated as cells exhibiting activated caspase-3 of all transfected (RFP+) cells.

(D) Apoptosis induced by increasing concentrations of anti-Fas antibody in 293T cells co-transfected with TRPM7 variants; Fas-induced apoptosis assessed by quantifying PARP cleavage in cell lysates. The graph shows average PARP cleavage indices (±SEM, n = 4).

(E) Ratiometric measurement of intracellular Ca^{2+} in LN18 cells transfected with indicated TRPM7 variants and loaded with fura-2 AM dye.

See also Figure S4.

The Cleavage of TRPM7 at D1510 Is Critical for the Potentiation of Fas-Induced Apoptosis by TRPM7

To evaluate the role of cleavage in extrinsic apoptosis, we investigated the ability of TRPM7 to potentiate Fas-induced apoptosis when the critical residue D1510 is mutated (TRPM7-D1510A or simply M7DA). We also evaluated the ability of the cleaved TRPM7 channel domain in this assay. Because the cleaved TRPM7 channel lacks the kinase domain, the TRPM7 variant truncated at D1510 is referred to as TRPM7-ΔK or M7-ΔK. We expressed the empty vector, M7-WT, M7-DA (TRPM7-D1510A mutant), M7ΔK (TRPM7 truncated at D1510), and M7ΔK-pm (nonconducting pore mutation in truncated TRPM7) in LN18 cells. Caspase cleavage-resistant M7D1510A mutant did not potentiate Fas-induced apoptosis, indicating that cleavage was necessary for this effect (Figures 4C and S4C). The cleaved channel greatly potentiated caspase-3 activation when the pore was functional (M7-ΔK), but not when the pore was mutated (M7-ΔK-pm) (Figures 4C and S4C). Similar results were obtained in 293T cells coexpressing the M7 variants and Fas, as measured by PARP cleavage (Figure 4D). Expression of M7ΔK but not M7D1510A or M7ΔK-pm increased the Fas sensitivity of 293T cells coexpressing the Fas receptor. Representative immunoblots of cleaved PARP and α-tubulin are shown in Figure S4D. The expression of TRPM7 variants and the Fas receptor is shown in Figure S4E. These results show that the critical TRPM7 function in Fas receptor signaling is dependent on cleavage-mediated modulation of TRPM7 channel activity but is not due to cellular Ca^{2+} overload. Although TRPM7 is a cationic channel permeant to Ca^{2+}, the inward conductance of TRPM7 at physiological membrane potential does not lead to a substantial influx of Ca^{2+} in cells expressing ectopic TRPM7 (Figure 4E). The precise mechanism by which TRPM7 modulates TRPM7 is not clear at this point but is likely to involve dynamic changes in subcellular microdomains of Ca^{2+}, Mg^{2+}, or Zn^{2+} during death receptor signaling.

Cleavage of TRPM7 at D1510 Increases TRPM7 Currents

The cleavage of TRPM7 at D1510 dissociates the 40 kDa kinase domain from the 172 kDa ion-conducting pore (M7-ΔK). To evaluate the effect of cleavage on TRPM7 channel conductance, we expressed TRPM7 variants in CHO cells. These cells have very low endogenous TRPM7 currents and allow electrophysiological resolution of I_{TRPM7} elicited by ectopically expressed TRPM7 variants without excessive overexpression. I_{TRPM7} characteristically develops over time after membrane rupture, a process commonly referred to as "break-in" during patch-clamp recording. All functional TRPM7 variants exhibited similar current-voltage relationships and were expressed at comparable levels in CHO cells (Figure S5A). We analyzed the mean

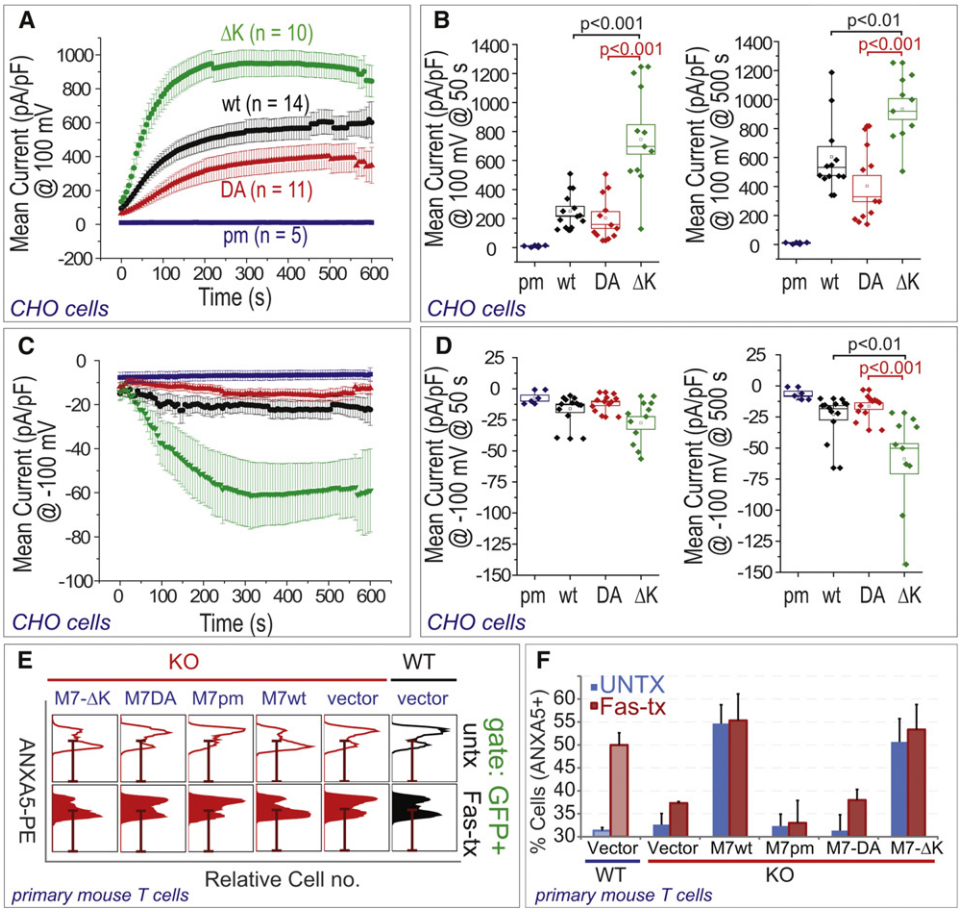

Figure 5. Cleavage of TRPM7 at D1510 Potentiates TRPM7 Currents

(A) I_{TRPM7} developed gradually with intracellular perfusion in CHO cells transfected with different TRPM7 variants. Current densities at +100mV are plotted against time after break-in.

(B) Box chart of TRPM7 maximum outward current densities at 50 s (left) and 500 s (right) after break-in (measured at +100mV). Statistics pertaining to TRPM7 currents are shown as Box (±SEM), vertical bars (5^{th}–95^{th} percentile), and data overlap.

(C) Maximum inward current densities (measured at −100mV).

(D) Box chart of inward current densities obtained at −100mV. See also Figure S5.

(E) The effect of ectopic expression of TRPM7 variants in KO T cells. The percentage of ANXA5+ T cells was quantified by flow cytometry (±SD, n = 3), and representative flow cytometry histograms are shown. The gating scheme is clarified in Figure S5.

(F) The bar graph shows quantitation of results as the percentage of ANXA5+ cells (±SD, n = 3) in T cells ectopically transfected with the indicated TRPM7 variants. See also Figure S5

current density in transfected CHO cells at +100mV (outward current, Figures 5A and 5B) and at −100mV (inward current, Figures 5C and 5D). In cells expressing M7-WT the current increases to a mean current density of 250 pA/pF after 50 s and to 600 pA/pF after 500 s, whereas M7-ΔK currents develop faster and exhibit mean current densities that are significantly higher (720 pA/pF after 50 s and 925 pA/pF after 500 s). In contrast, cells transfected with M7-pm lack substantial current after break-in (Figures 5A and 5B, blue). TRPM7-D1510A (M7-DA) current densities are somewhat lower, but not significantly different than WT. In agreement with a previous report by Schmitz et al. (2003), point mutations that inactivated the kinase did not affect TRPM7 channel activity (Figures S5B and S5C). Overall, these data indicate that after the cleavage of TRPM7 by caspase-8, higher currents are achieved when compared to full length, uncleaved TRPM7.

We also confirmed that I_{TRPM7} is expressed in LN18 cells. A Mg^{2+}-inhibitable current develops in a time-dependent manner (Figure S5D) and shows the signature current-voltage relationship of I_{TRPM7}. Furthermore, we show that this current shows pharmacological sensitivity identical to that of TRPM7. It is inhibited by 0.5 mM 2APB but fully reactivated by 2 mM 2APB (Figure S5E). I_{TRPM7} in LN18 cells is also activated by 10 mM NH_4Cl (data not shown).

Reconstitution of TRPM7 Variants in *Trpm7*$^{-/-}$ Mouse T Cells

Next, we evaluated the effect of reconstituting TRPM7 variants in *Trpm7*$^{-/-}$ T cells. In comparison to WT T cells, the vector-transfected *Trpm7*$^{-/-}$ T cells were less than half as sensitive to FAS stimulation (Figures 5E, 5F, and S5D). Surprisingly, the *Trpm7*$^{-/-}$ T cells transfected with TRPM7-WT and TRPM7-ΔK exhibited

spontaneous (without FAS stimulation) apoptosis. This effect was not seen in cells expressing TRPM7-pm and TRPM7-DA, suggesting that *Trpm7*$^{-/-}$ T cells are capable of apoptosis but are restrained due to a lack of TRPM7 channel activity. Overexpression of competent TRPM7 variants likely leads to apoptosis due to the presence of active caspases in proliferating T cells (Kennedy et al., 1999; Leverrier et al., 2011; Siegel, 2006). Because TRPM7-pm and TRPM7-DA do not result in apoptosis, the results support the conclusion that the cleavage of TRPM7 at D1510 and the consequent channel activity plays an important role in FAS-induced apoptosis.

TRPM7 Acts Upstream of Cytochrome *c* Release during Fas-Induced Apoptosis

For mechanistic insight and to pinpoint the process that is regulated by TRPM7 during Fas-induced apoptosis, we first determined whether TRPM7 acts upstream or downstream of cytochrome *c* release from mitochondria in LN18 cells. We generated a stable cell line, *LN18 (CytC-GFP)*, expressing cytochrome *c*-GFP in the LN18 background. In this cell line, cytochrome *c*-GFP localizes predictably to the mitochondria and is released from the mitochondria in response to Fas stimulation (Movie S1). When these cells are transfected with siRNA targeting TRPM7, the release of cytochrome *c*-GFP from the mitochondria is abrogated (Figures 6A and 6B). After 180 min of Fas stimulation, 37% of the cells transfected with control siRNA released cytochrome *c*. In contrast only 5% of the cells transfected with TRPM7 siRNA released cytochrome *c*-GFP (Figure 6B). A similar difference was seen at 240 min of Fas stimulation (Figure 6B). These data indicate that TRPM7 acts upstream of cytochrome *c* release in type 2 cells. We also evaluated the effect of knocking down TRPM7 in SKW6.4 cells, a prototypical type 1 Fas-sensitive cell line that does not depend on the mitochondrial amplification loop to execute Fas-induced apoptosis (Schmitz et al., 1999). The reduction in TRPM7 levels upon transfection of TRPM7-targeting siRNA is shown through immunoprecipitation and immunoblotting of TRPM7 (Figure S6A). SKW6.4 cells with reduced TRPM7 levels show significantly reduced sensitivity to Fas-induced apoptosis (Figure S6B).

TRPM7 Does Not Regulate Formation of the DISC

We analyzed the DISC in SKW6.4 cells with knocked down TRPM7 in consideration of the hypothesis that TRPM7 regulates the assembly of the DISC upon Fas stimulation. This was done by immunoprecipitating the Fas receptor from lysates generated at specific time points after Fas stimulation and immunoblotting for the two key components of DISC: procaspase-8 and FADD. These results, shown in Figure 6C, do not support the hypothesis that TRPM7 regulates the assembly of DISC. After 10 min of Fas stimulation, both cell populations (control siRNA and TRPM7 siRNA-treated) show recruitment of FADD and procaspase-8. The composition of DISC at 60 min shows modest differences in the levels of procaspase-8, but our results did not allow us to conclude that this difference was statistically significant. Interestingly, the activity of caspase-8 at the same time points shows modest but significant differences (Figure 6D). These data indicate that although TRPM7 does not regulate the assembly of DISC, it influences the processing of caspase-8 in the subsequent steps. Fas receptor transmits apoptotic as well as survival signals (Peter et al., 2007). The process by which the cellular context dictates whether Fas signaling results in apoptosis or nonapoptotic signals is not well understood, but internalization and compartmentalization of the DISC have been proposed as critical events driving the transmission of apoptotic signal (Schütze et al., 2008). In SKW6.4 cells transfected with TRPM7 siRNA, we observed that decreased sensitivity to apoptosis (Figures 6E and S6B) was also accompanied by activation of the MAPK pathway, as detected by the presence of phosphorylated Erk1/Erk2 in cell lysates (Figure 6E). We then considered the possibility that SKW6.4 cells with reduced TRPM7 were compromised in the process of Fas receptor endocytosis after Fas stimulation, favoring the transmission of nonapoptotic signals downstream of Fas.

TRPM7 Regulates Internalization of Fas following Receptor Stimulation

Internalization of the Fas receptor in SKW6.4 cells following receptor stimulation has been described previously (Algeciras-Schimnich et al., 2002; Siegel et al., 2004). We used an anti-Fas agonist antibody conjugated to a fluorophore (Alexa 568) to stimulate the Fas receptor and observe its subsequent internalization. The staining of the Fas receptor (on the cell surface) with this antibody is detectable after 15 min of incubation in cell culture conditions. As shown in Figure S6C, internalization follows this receptor engagement, and 75% of the SKW6.4 cells can be seen to have internalized the Fas receptor after 1 hr of stimulation (Figures 6F and 6G). In contrast, the SKW6.4 cells that are transfected with TRPM7 siRNA do not exhibit Fas internalization at a comparable level; only 30% of the cells show Fas internalization (Figures 6F and 6G). We carried out the same experiment with LN18 cells. In the case of LN18 cells, the Fas receptor levels are lower, and their distribution in the plasma membrane was strikingly polarized. Nevertheless, internalization is readily detectable in LN18 cells transfected with control siRNA. Again, the cells transfected with TRPM7 siRNA show considerably reduced incidence of Fas receptor internalization after 1 hr of stimulation (Figures 6H and 6I). A time course of internalization in the LN18 cells is shown in Figure S6D as a montage of images acquired between 15 min and 1 hr of Fas stimulation. The punctate pattern of internalized Fas is not due to redistribution of the Fas receptor within the plasma membrane—the punctae are indeed inside the cells. This is demonstrated through the acquisition of confocal images along the vertical axis (z stack of images) of cells transfected with control siRNA and TRPM7 siRNA. These images are shown as a combined movie (Movie S2). Overall, these results clearly show that TRPM7 participates in regulating the internalization of Fas receptor.

Lung Inflammation and Airspace Enlargement in Aged $T^{M7-/-}$ Mice

$T^{M7-/-}$ mice show a pathophysiological similarity to the mice in which the Fas receptor is selectively deleted in T cells ($T^{Fas-/-}$ mice). In contrast to the phenotype of global deletion of Fas, which results in lymphoproliferative, autoimmune pathology in young animals (Watanabe-Fukunaga et al., 1992), the selective deletion of Fas in T cells leads to lymphopenia and a high incidence of pulmonary inflammation and lung-tissue damage upon aging (Hao et al., 2004). Similarly, the lungs of 13- to

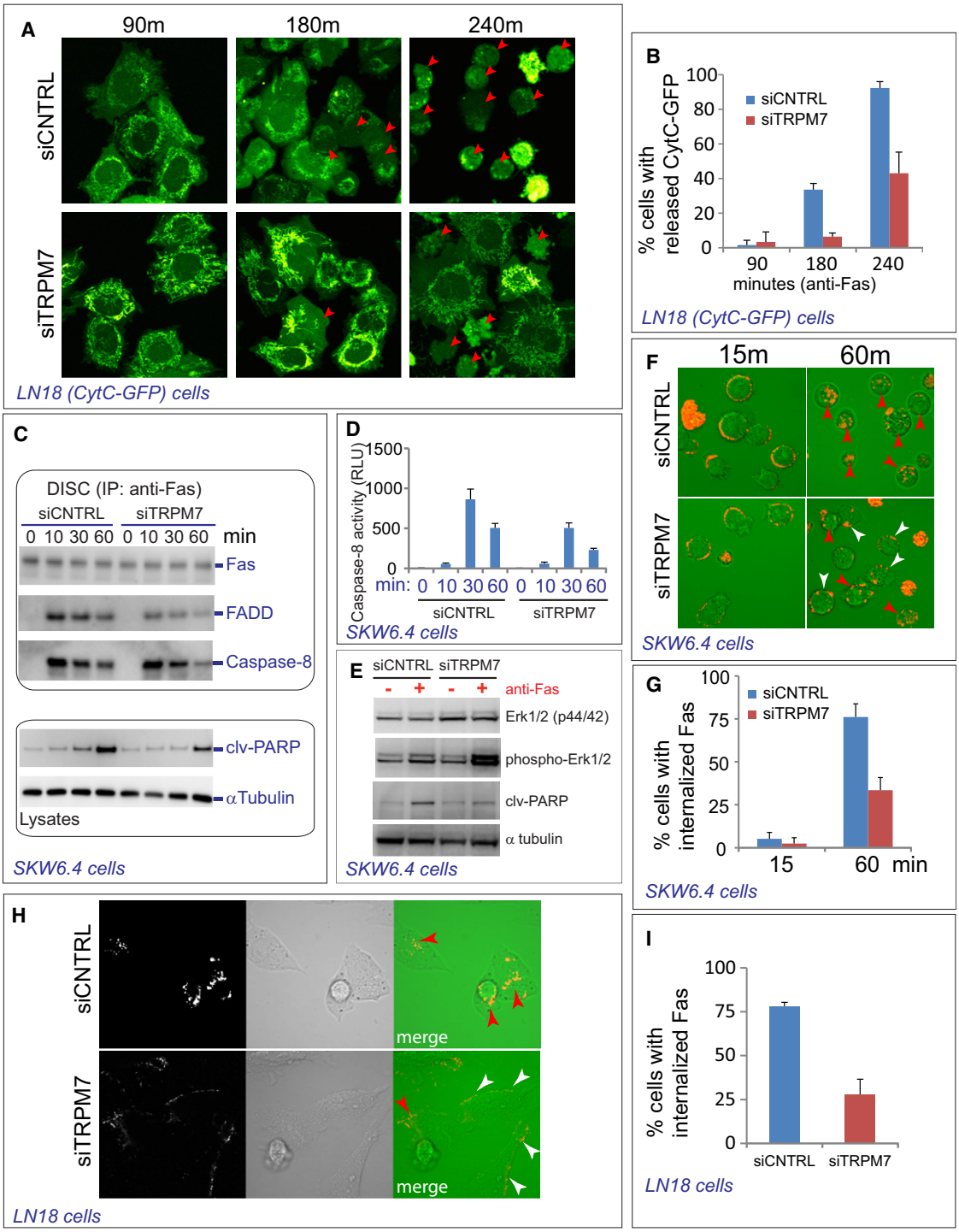

Figure 6. TRPM7 Regulates Internalization of Fas Receptor

(A) LN18 cells stably transfected with CytC-GFP were transfected with indicated siRNA. Release of cytochrome *c* was evaluated upon Fas stimulation at indicated time points. Red arrowheads mark the cells that have released CytC-GFP from the mitochondria.

(B) Quantitation of cytochrome *c* release is shown as percentage of cells with released CytC-GFP at indicated time points after Fas stimulation.

(C) Top shows analysis of DISC formation at indicated time points after Fas stimulation in SKW6.4 cells. Immunoblots show the levels of Fas, FADD, and caspase-8 in isolated DISC. Bottom shows levels of cleaved PARP and α-tubulin in the lysates of Fas-stimulated SKW6.4 cells at corresponding times shown in the top panel.

(D) Caspase-8 activity in caspase-8 immunoprecipitates isolated from Fas-stimulated SKW6.4 cells at indicated time points. The y axis shows relative luminescence units (RLU) detected upon cleavage of luminogenic caspase-8 substrate in presence of luciferase enzyme.

(E) Immunoblots show the presence of phosphor-Erk1/Erk2 in the lysates of unstimulated and Fas-stimulated (1 hr) SKW6.4 cells.

15-month-old $T^{M7-/-}$ mice exhibit pulmonary inflammation and emphysema. Hematoxylin and eosin staining (H&E) of lung tissues revealed alveolar damage and significant enlargement of alveolar airspaces, similar to the histopathology of emphysema (Figure 7A). We quantified the enlargement of alveolar airspaces through morphometric analysis (Jacob et al., 2009) of H&E lung slices of WT and $T^{M7-/-}$ as briefly illustrated in Figure S7. A comparison of mean linear intercept (MLI) and the statistical moments (D_0, D_1, and D_2) of the equivalent diameter (d_{eq}) between the airspaces of WT and $T^{M7-/-}$ mice lungs are shown as statistical box charts in Figure 7B. Antibody staining using anti-CD3 (Figure 7C, left), B220 (Figure 7C, right), and Ly6G (Figure 7D) documents the increased infiltration of T cells, B cells, and neutrophils into the lungs of aged $T^{M7-/-}$ mice (Figure 7E). We did not observe a significant difference between the lungs of young mice, suggesting that pulmonary inflammation and emphysema seen in the $T^{M7-/-}$ mice are age dependent. This is remarkably similar to the phenotype of mice in which Fas was selectively deleted in T cells. The selective deletion of Fas in T cells leads to lymphopenia without obvious pathology in young mice, but a high incidence of pulmonary inflammation and lung-tissue damage upon aging (Hao et al., 2004). This phenotype is distinct from global deletion of Fas, which results in an autoimmune pathology that is evident in young animals (Watanabe-Fukunaga et al., 1992).

DISCUSSION

We demonstrated that TRPM7 is cleaved by caspase-8 at D1510, dissociating the kinase from the ion-conducting pore. The cleaved channel exhibits substantially higher I_{TRPM7} and potentiates Fas receptor signaling. In contrast, neither the cleaved kinase domain nor the cleavage-resistant TRPM7 D1510A mutant potentiates this pathway. Cleavage-induced current enhancement is specific to D1510 because TRPM7 truncated at other sites within the kinase domain does not elicit an increase in currents (Matsushita et al., 2005; Schmitz et al., 2003). The cleavage-induced augmentation of TRPM7 channel activity is not due to inactivation of its kinase. Cleavage elicits two distinct functional proteins (channel and kinase) that can now differentially localize. These data indicate that TRPM7 cleavage is an important regulatory step for TRPM7 function in Fas receptor signaling. In cells where TRPM7 levels have been reduced substantially through siRNA treatment, the Fas receptor is not internalized normally in response to receptor stimulation. In these cells, the reduction in their sensitivity to Fas-induced apoptosis correlates with an increase in activation of MAPK pathway, a nonapoptotic signaling route for Fas signaling. Finally, in accord with the cellular phenotype, the $T^{M7-/-}$ mice show a distinct pathophysiological similarity to the mice in which Fas is selectively deleted in T cells ($T^{Fas-/-}$ mice).

Because many TRP channels have emerged as regulators of cell death (Aarts et al., 2003; Hara et al., 2002), inflammation (Barbet et al., 2008; Link et al., 2010; Sumoza-Toledo and Penner, 2011; Yamamoto et al., 2008), and pain (Basbaum et al., 2009), this study raises the possibility that in these roles, TRP channels are regulated through caspase-mediated cleavage events. The findings thus offer an avenue of research to guide pharmacological intervention of multiple diseases.

EXPERIMENTAL PROCEDURES

Reagents and detailed methods are in the Supplemental Experimental Procedures.

Mice

Mice were bred and maintained according to guidelines and procedures approved by the Institutional Animal Care and Use Committee.

Cell Culture

HEK293, LN18, Jurkat (clone E6-1), CHO, and SKW6.4 cell lines were obtained from American Type Culture Collection (ATCC). Fas receptor stimulation for indicated times was with anti-human Fas antibody (clone CH11). Primary mouse T cells were activated using bead-bound anti-CD3 and anti-CD28 in the presence of 50 U/ml recombinant mouse IL-2 and maintained at a concentration of 0.5–0.75 million cells/ml in RPMI growth medium supplemented with 10% FBS, 1 mM glutamine, and 0.001% 2-mercaptoethanol. Fas receptors were activated by anti-mouse Fas (CD95) Jo2 clone in 0.5 μg/ml Protein G. Alternatively, apoptosis was induced by culturing T cells with plate-bound (10 μg/ml) anti-Fas antibody (see Supplemental Experimental Procedures).

Biochemical Analysis of TRPM7 Cleavage

LN18 cells were lysed in ice-cold lysis buffer (20 mM Tris-HCl, 150 mM NaCl, 1.0% Triton X-100 [pH 8.0]) containing protease and phosphatase inhibitor cocktail (Pierce). Immunoprecipitations were carried out using the C47 antibody (2 μg/ml) or N74/25 antibody (50 μl hybridoma supernatant/ml) at 4°C for 12–16 hr. TRPM7 was detected by immunoblotting with C-47 antibody (2 μg/ml). For in vitro cleavage, the ^{35}S-labeled TRPM7 C-terminal polypeptide sequences (aa 1,364–1,863) were synthesized in vitro using the TNT-T7 (Promega). A total of 2 μl of reaction mixture containing the ^{35}S-labeled polypeptide was incubated with 2 U of purified caspase-8 in 15 μl of AMC buffer (20 mM PIPES [pH 7.2], 100 mM NaCl, 1 mM EDTA, 0.1% CHAPS, 10% sucrose, 10 mM DTT, 1 mg/ml Pefablock SC) at 37°C for 2.5 hr prior to analysis by electrophoresis and autoradiography. See Supplemental Experimental Procedures for additional methods pertaining to biochemical analysis of TRPM7 cleavage.

DISC Analysis

SKW6.4 cells were stimulated with 2 μg/ml of anti-Fas antibody (clone APO-1-1; Kamiya Biomedical) at 37°C and lysed at indicated time points. The lysis buffer (30 mM Tris-HCl [pH 7.4], 150 mM NaCl, 1% Triton X-100, and 10% glycerol) was supplemented with protease inhibitor cocktail (Roche) immediately before use. For the untreated or 0 min condition, antibody was added after lysis of unstimulated cells. The DISC (Fas immunoprecipitate) was

(F) The confocal images show internalization of Fas in SKW6.4 cells after Fas stimulation with Alexa 568-conjugated anti-Fas antibody. The images shown are mergers of red channel (Alexa 568) and differential interference contrast (DIC) (shown in green for better contrast). Red arrowheads mark the cells with internalized Fas, and white arrowheads mark the cells with Fas at the plasma membrane (not internalized).
(G) The bar graphs show the percentage of cells with internalized Fas in SKW6.4 cells at indicated time points, as detected microscopically.
(H) Confocal images show internalization of Fas in LN18 cells after Fas stimulation (1 hr) with Alexa 568-conjugated anti-Fas antibody. The images are of Alexa 568-labeled cells in fluorescence and DIC; merged images show Alexa 568 in red (appears orange in merged image) and DIC in green for contrast. Red arrowheads mark the cells with internalized Fas, and white arrowheads mark the cells with Fas at the plasma membrane (not internalized).
(I) The bar graphs show the percentage of LN18 cells with internalized Fas after 1 hr of Fas stimulation as detected microscopically.
See also Figure S6 and Movie S2.

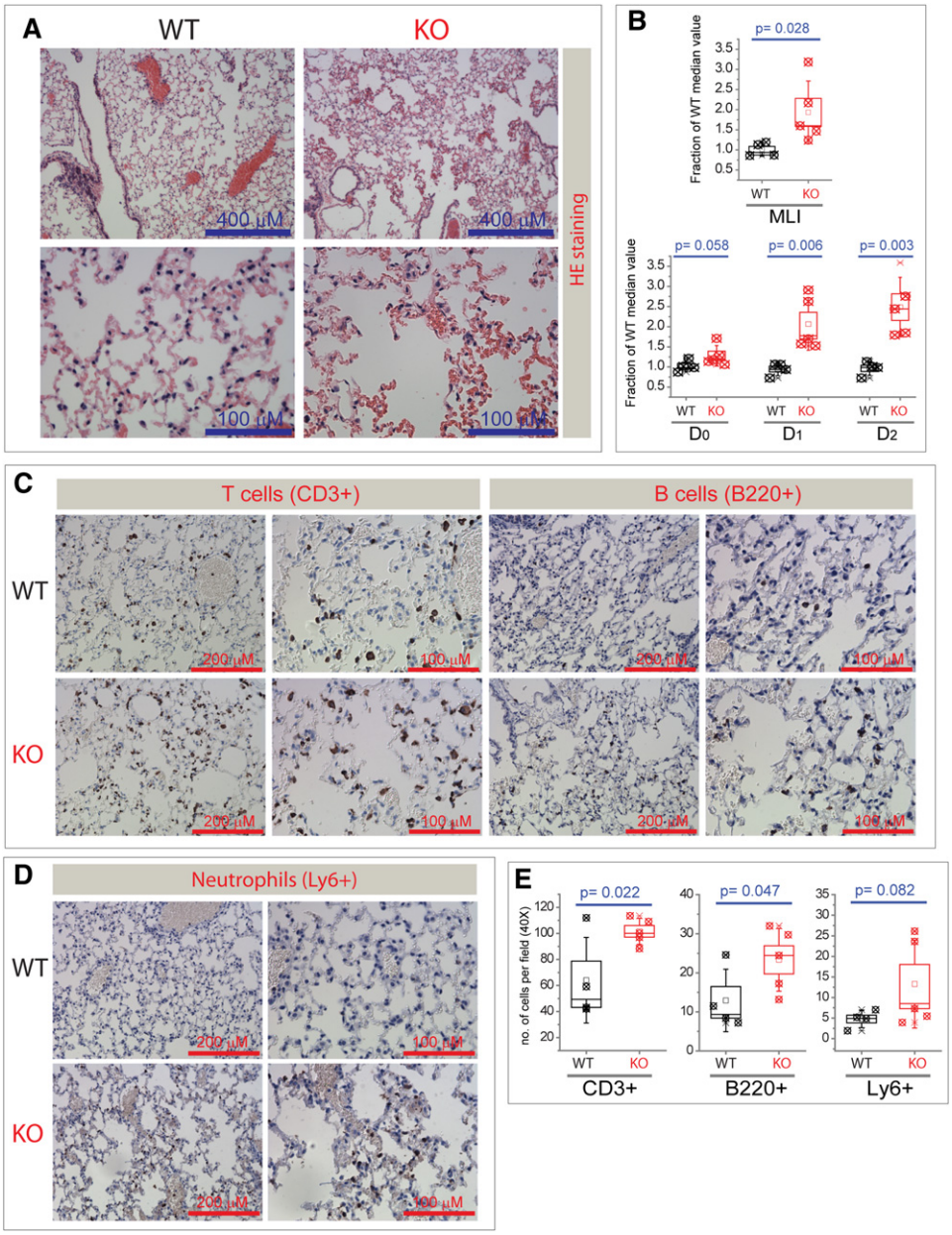

Figure 7. Lung Inflammation and Airspace Enlargement in *M7*$^{-/fl}$ *(lck-Cre)* Mice

(A) H&E of lung sections from WT and *M7*$^{-/fl}$ *(lck-Cre)* (KO) mice.

(B) Statistical box charts of lung morphometric measurements comparing the alveolar airspaces in WT and *KO* lungs. Each data point in the box charts denotes a measurement from a lung sample derived from a distinct mouse. The minimum number of airspace areas analyzed per lung sample was 47; total airspace area analyzed was 693 (WT) and 446 (*KO*). Top panel presents calculated MLI, a metric of airspace enlargement (see Experimental Procedures). Bottom panel illustrates d_{eq} of calculated airspace areas. The image-processing steps and calculations used to calculate these parameters are illustrated in Figure S3 and detailed in Supplemental Experimental Procedures.

(C) Representative images of IHC-stained lung sections from WT and *M7*$^{-/fl}$ *(lck-Cre)* (*KO*) mice. The T cells (left panels) were stained using the anti-CD3 antibody, and the B cells (right panels) were stained using the anti-B220 antibody.

(D) Immunohistochemical detection of neutrophils (anti-Ly6 antibody).

(E) Box charts quantifying cells found in a microscopic field (40×). Statistics pertaining to lung pathology are shown as Box (±SEM), vertical bars (±SD), and data overlap.

See also Figure S7.

isolated by incubating the lysates with protein A Sepharose for 2 hr at 4°C and washed with lysis buffer prior to separation by SDS-PAGE and immunoblotting. For caspase-8 assays, the lysis buffer was supplemented with 0.5 μM MG-132 protease inhibitor. Caspase-8 was immunoprecipitated from lysates and washed thoroughly in the lysis buffer prior to activity assays. The immunoprecipitated pellets were resuspended in caspase-Glo 8 reagent (Promega).

The cleavage reactions were incubated for 30 min at room temperature, and relative luminescence was measured. siRNA cocktail was composed of 5 nM M7siR#2 and 5 nM M7siR#3 (see Supplemental Experimental Procedures).

Fas Internalization

Cells plated in glass-bottomed dishes were cultured in synthetic serum-free medium (Opti-MEM; Invitrogen) for 6 hr prior to internalization assays. Cells were incubated with 2 μg/ml Alexa 568-conjugated anti-Fas antibody (CH11 clone; Millipore) for 15 min in cell culture conditions (antibody-binding phase). The cells were washed in Opti-MEM (37°C) and images acquired using an Olympus FV1000 confocal microscope (maintained at 37°C during imaging). siRNA cocktail was composed of 5 nM M7siR#2 and 5 nM M7siR#3 (see Supplemental Experimental Procedures).

Electrophysiology

In case of CHO cells, standard bath solution contained 135 mM Na-methanesulfonate (Na-$MeSO_3$), 5 mM CsCl, 1 mM $CaCl_2$, 10 mM HEPES (pH 7.4) with NaOH. The standard pipette solution was 120 mM Cs-$MeSO_3$, 5 mM CsCl, 10 mM BAPTA, 3.1 mM $CaCl_2$, 3 mM ATP-Na, 0.6 mM GTP-Na, 10 mM HEPES (pH 7.2) with CsOH. Signals were sampled at 10 Khz and low-pass filtered at 2 kHz. For Jurkat cells and LN18 cells, the modified methods are described in the Supplemental Experimental Procedures. In shRNA-treated Jurkat cells, the TRPM7-dependent component of outward current (I_{MIC}) was defined by superfusion of 5 mM extracellular Mg^{2+} to block I_{MIC}. Currents were measured at +100mV following voltage ramps from −100mV; holding potential was 0mV.

Histology and Immunohistochemistry

Immediately after euthanizing 13- to 15-month-old mice, the lungs were inflated and fixed by intratracheal instillation of freshly prepared 5% buffered PFA, excised, and immersed in the same fixative for 24 hr. The fixed tissue samples were embedded in paraffin, sectioned into 4–6 μm slices, and H&E. Immunohistochemistry (IHC) experiments were in formalin-fixed, paraffin-embedded tissue sections (see Supplemental Experimental Procedures). See Figure S7 and Supplemental Experimental Procedures for lung morphometric measurements.

Box Charts and Statistics

Statistics pertaining to the lung pathology are shown as Box (±SEM), vertical bars (±SD), and data overlap. Statistics pertaining to TRPM7 currents are shown as box (±SEM), vertical bars (5^{th}–95^{th} percentile), and data overlap. All individual data points are shown; the mean value is denoted by an empty square, and the median is shown as a horizontal line. p values were calculated using Student's t test and ANOVA.

SUPPLEMENTAL INFORMATION

Supplemental Information includes seven figures, Supplemental Experimental Procedures, and two movies and can be found with this article online at doi:10.1016/j.devcel.2012.04.006.

ACKNOWLEDGMENTS

We thank Jie Jin for assistance regarding *Trpm7-targeted* mice, Andrew Scharenberg (University of Washington) for the 293T cell line expressing FLAG-tagged TRPM7, Douglas Green (St. Jude Children's Research Hospital) for the cytochrome *c*-GFP plasmid, Grigoriy Losiyev (Brigham and Women's Hospital [BWH]) for flow cytometry, the BWH Histopathology core, and Clapham laboratory members for helpful discussions.

Received: October 12, 2011
Revised: March 13, 2012
Accepted: April 11, 2012
Published online: June 11, 2012

REFERENCES

Aarts, M., Iihara, K., Wei, W.L., Xiong, Z.G., Arundine, M., Cerwinski, W., MacDonald, J.F., and Tymianski, M. (2003). A key role for TRPM7 channels in anoxic neuronal death. Cell *115*, 863–877.

Algeciras-Schimnich, A., Shen, L., Barnhart, B.C., Murmann, A.E., Burkhardt, J.K., and Peter, M.E. (2002). Molecular ordering of the initial signaling events of CD95. Mol. Cell. Biol. *22*, 207–220.

Barbet, G., Demion, M., Moura, I.C., Serafini, N., Léger, T., Vrtovsnik, F., Monteiro, R.C., Guinamard, R., Kinet, J.P., and Launay, P. (2008). The calcium-activated nonselective cation channel TRPM4 is essential for the migration but not the maturation of dendritic cells. Nat. Immunol. *9*, 1148–1156.

Basbaum, A.I., Bautista, D.M., Scherrer, G., and Julius, D. (2009). Cellular and molecular mechanisms of pain. Cell *139*, 267–284.

Brauchi, S., Krapivinsky, G., Krapivinsky, L., and Clapham, D.E. (2008). TRPM7 facilitates cholinergic vesicle fusion with the plasma membrane. Proc. Natl. Acad. Sci. USA *105*, 8304–8308.

Clark, K., Middelbeek, J., Lasonder, E., Dulyaninova, N.G., Morrice, N.A., Ryazanov, A.G., Bresnick, A.R., Figdor, C.G., and van Leeuwen, F.N. (2008). TRPM7 regulates myosin IIA filament stability and protein localization by heavy chain phosphorylation. J. Mol. Biol. *378*, 790–803.

Demeuse, P., Penner, R., and Fleig, A. (2006). TRPM7 channel is regulated by magnesium nucleotides via its kinase domain. J. Gen. Physiol. *127*, 421–434.

Dorovkov, M.V., and Ryazanov, A.G. (2004). Phosphorylation of annexin I by TRPM7 channel-kinase. J. Biol. Chem. *279*, 50643–50646.

Green, D.R., Droin, N., and Pinkoski, M. (2003). Activation-induced cell death in T cells. Immunol. Rev. *193*, 70–81.

Hao, Z., Hampel, B., Yagita, H., and Rajewsky, K. (2004). T cell-specific ablation of Fas leads to Fas ligand-mediated lymphocyte depletion and inflammatory pulmonary fibrosis. J. Exp. Med. *199*, 1355–1365.

Hara, Y., Wakamori, M., Ishii, M., Maeno, E., Nishida, M., Yoshida, T., Yamada, H., Shimizu, S., Mori, E., Kudoh, J., et al. (2002). LTRPC2 Ca2+-permeable channel activated by changes in redox status confers susceptibility to cell death. Mol. Cell *9*, 163–173.

Jacob, R.E., Carson, J.P., Gideon, K.M., Amidan, B.G., Smith, C.L., and Lee, K.M. (2009). Comparison of two quantitative methods of discerning airspace enlargement in smoke-exposed mice. PLoS One *4*, e6670.

Jiang, J., Li, M., and Yue, L. (2005). Potentiation of TRPM7 inward currents by protons. J. Gen. Physiol. *126*, 137–150.

Jin, J., Desai, B.N., Navarro, B., Donovan, A., Andrews, N.C., and Clapham, D.E. (2008). Deletion of Trpm7 disrupts embryonic development and thymopoiesis without altering Mg2+ homeostasis. Science *322*, 756–760.

Jin, J., Wu, L.J., Jun, J., Cheng, X., Xu, H., Andrews, N.C., and Clapham, D.E. (2012). The channel kinase, TRPM7, is required for early embryonic development. Proc. Natl. Acad. Sci. USA *109*, E225–E233.

Kaiser, W.J., Upton, J.W., Long, A.B., Livingston-Rosanoff, D., Daley-Bauer, L.P., Hakem, R., Caspary, T., and Mocarski, E.S. (2011). RIP3 mediates the embryonic lethality of caspase-8-deficient mice. Nature *471*, 368–372.

Kennedy, N.J., Kataoka, T., Tschopp, J., and Budd, R.C. (1999). Caspase activation is required for T cell proliferation. J. Exp. Med. *190*, 1891–1896.

Kozak, J.A., and Cahalan, M.D. (2003). MIC channels are inhibited by internal divalent cations but not ATP. Biophys. J. *84*, 922–927.

Krammer, P.H., Arnold, R., and Lavrik, I.N. (2007). Life and death in peripheral T cells. Nat. Rev. Immunol. *7*, 532–542.

Krapivinsky, G., Mochida, S., Krapivinsky, L., Cibulsky, S.M., and Clapham, D.E. (2006). The TRPM7 ion channel functions in cholinergic synaptic vesicles and affects transmitter release. Neuron *52*, 485–496.

Kunert-Keil, C., Bisping, F., Krüger, J., and Brinkmeier, H. (2006). Tissue-specific expression of TRP channel genes in the mouse and its variation in three different mouse strains. BMC Genomics *7*, 159.

Langeslag, M., Clark, K., Moolenaar, W.H., van Leeuwen, F.N., and Jalink, K. (2007). Activation of TRPM7 channels by phospholipase C-coupled receptor agonists. J. Biol. Chem. *282*, 232–239.

Leverrier, S., Salvesen, G.S., and Walsh, C.M. (2011). Enzymatically active single chain caspase-8 maintains T-cell survival during clonal expansion. Cell Death Differ. *18*, 90–98.

Li, F.Y., Chaigne-Delalande, B., Kanellopoulou, C., Davis, J.C., Matthews, H.F., Douek, D.C., Cohen, J.I., Uzel, G., Su, H.C., and Lenardo, M.J. (2011). Second messenger role for Mg2+ revealed by human T-cell immunodeficiency. Nature *475*, 471–476.

Li, H., Zhu, H., Xu, C.J., and Yuan, J. (1998). Cleavage of BID by caspase 8 mediates the mitochondrial damage in the Fas pathway of apoptosis. Cell *94*, 491–501.

Li, P., Nijhawan, D., Budihardjo, I., Srinivasula, S.M., Ahmad, M., Alnemri, E.S., and Wang, X. (1997). Cytochrome c and dATP-dependent formation of Apaf-1/caspase-9 complex initiates an apoptotic protease cascade. Cell *91*, 479–489.

Link, T.M., Park, U., Vonakis, B.M., Raben, D.M., Soloski, M.J., and Caterina, M.J. (2010). TRPV2 has a pivotal role in macrophage particle binding and phagocytosis. Nat. Immunol. *11*, 232–239.

Liu, X., Kim, C.N., Yang, J., Jemmerson, R., and Wang, X. (1996). Induction of apoptotic program in cell-free extracts: requirement for dATP and cytochrome c. Cell *86*, 147–157.

Lowe, S.W., Ruley, H.E., Jacks, T., and Housman, D.E. (1993). p53-dependent apoptosis modulates the cytotoxicity of anticancer agents. Cell *74*, 957–967.

Mahrus, S., Trinidad, J.C., Barkan, D.T., Sali, A., Burlingame, A.L., and Wells, J.A. (2008). Global sequencing of proteolytic cleavage sites in apoptosis by specific labeling of protein N termini. Cell *134*, 866–876.

Matsushita, M., Kozak, J.A., Shimizu, Y., McLachlin, D.T., Yamaguchi, H., Wei, F.Y., Tomizawa, K., Matsui, H., Chait, B.T., Cahalan, M.D., and Nairn, A.C. (2005). Channel function is dissociated from the intrinsic kinase activity and autophosphorylation of TRPM7/ChaK1. J. Biol. Chem. *280*, 20793–20803.

McStay, G.P., Salvesen, G.S., and Green, D.R. (2008). Overlapping cleavage motif selectivity of caspases: implications for analysis of apoptotic pathways. Cell Death Differ. *15*, 322–331.

Nadler, M.J., Hermosura, M.C., Inabe, K., Perraud, A.L., Zhu, Q., Stokes, A.J., Kurosaki, T., Kinet, J.P., Penner, R., Scharenberg, A.M., and Fleig, A. (2001). LTRPC7 is a Mg.ATP-regulated divalent cation channel required for cell viability. Nature *411*, 590–595.

Oberst, A., Dillon, C.P., Weinlich, R., McCormick, L.L., Fitzgerald, P., Pop, C., Hakem, R., Salvesen, G.S., and Green, D.R. (2011). Catalytic activity of the caspase-8-FLIP(L) complex inhibits RIPK3-dependent necrosis. Nature *471*, 363–367.

Peter, M.E., Budd, R.C., Desbarats, J., Hedrick, S.M., Hueber, A.O., Newell, M.K., Owen, L.B., Pope, R.M., Tschopp, J., Wajant, H., et al. (2007). The CD95 receptor: apoptosis revisited. Cell *129*, 447–450.

Pop, C., and Salvesen, G.S. (2009). Human caspases: activation, specificity, and regulation. J. Biol. Chem. *284*, 21777–21781.

Ramsey, I.S., Delling, M., and Clapham, D.E. (2006). An introduction to TRP channels. Annu. Rev. Physiol. *68*, 619–647.

Romani, A.M., and Scarpa, A. (2000). Regulation of cellular magnesium. Front. Biosci. *5*, D720–D734.

Runnels, L.W., Yue, L., and Clapham, D.E. (2001). TRP-PLIK, a bifunctional protein with kinase and ion channel activities. Science *291*, 1043–1047.

Runnels, L.W., Yue, L., and Clapham, D.E. (2002). The TRPM7 channel is inactivated by PIP(2) hydrolysis. Nat. Cell Biol. *4*, 329–336.

Ryazanova, L.V., Rondon, L.J., Zierler, S., Hu, Z., Galli, J., Yamaguchi, T.P., Mazur, A., Fleig, A., and Ryazanov, A.G. (2010). TRPM7 is essential for Mg(2+) homeostasis in mammals. Nat. Commun. *1*, 109.

Schmitz, C., Perraud, A.L., Johnson, C.O., Inabe, K., Smith, M.K., Penner, R., Kurosaki, T., Fleig, A., and Scharenberg, A.M. (2003). Regulation of vertebrate cellular Mg2+ homeostasis by TRPM7. Cell *114*, 191–200.

Schmitz, I., Walczak, H., Krammer, P.H., and Peter, M.E. (1999). Differences between CD95 type I and II cells detected with the CD95 ligand. Cell Death Differ. *6*, 821–822.

Schütze, S., Tchikov, V., and Schneider-Brachert, W. (2008). Regulation of TNFR1 and CD95 signalling by receptor compartmentalization. Nat. Rev. Mol. Cell Biol. *9*, 655–662.

Siegel, R.M. (2006). Caspases at the crossroads of immune-cell life and death. Nat. Rev. Immunol. *6*, 308–317.

Siegel, R.M., Muppidi, J.R., Sarker, M., Lobito, A., Jen, M., Martin, D., Straus, S.E., and Lenardo, M.J. (2004). SPOTS: signaling protein oligomeric transduction structures are early mediators of death receptor-induced apoptosis at the plasma membrane. J. Cell Biol. *167*, 735–744.

Sumoza-Toledo, A., and Penner, R. (2011). TRPM2: a multifunctional ion channel for calcium signalling. J. Physiol. *589*, 1515–1525.

Watanabe-Fukunaga, R., Brannan, C.I., Copeland, N.G., Jenkins, N.A., and Nagata, S. (1992). Lymphoproliferation disorder in mice explained by defects in Fas antigen that mediates apoptosis. Nature *356*, 314–317.

Yamaguchi, H., Matsushita, M., Nairn, A.C., and Kuriyan, J. (2001). Crystal structure of the atypical protein kinase domain of a TRP channel with phosphotransferase activity. Mol. Cell *7*, 1047–1057.

Yamamoto, S., Shimizu, S., Kiyonaka, S., Takahashi, N., Wajima, T., Hara, Y., Negoro, T., Hiroi, T., Kiuchi, Y., Okada, T., et al. (2008). TRPM2-mediated Ca2+influx induces chemokine production in monocytes that aggravates inflammatory neutrophil infiltration. Nat. Med. *14*, 738–747.

Zhou, H., and Clapham, D.E. (2009). Mammalian MagT1 and TUSC3 are required for cellular magnesium uptake and vertebrate embryonic development. Proc. Natl. Acad. Sci. USA *106*, 15750–15755.